Available online at www.sciencedirect.com

ScienceDirect

MATTER AND RADIATION AT EXTREMES

Matter and Radiation at Extremes 3 (2018) 293–299

www.journals.elsevier.com/matter-and-radiation-at-extremes

Research Article

Characteristics of X/γ-ray radiations by intense laser interactions with high-Z solids: The role of bremsstrahlung and radiation reactions

D. Wu [a,b,*], W. Yu [a], Y.T. Zhao [b], S. Fritzsche [c,d], X.T. He [e]

[a] State Key Laboratory of High Field Laser Physics, Shanghai Institute of Optics and Fine Mechanics, 201800 Shanghai, China
[b] College of Science, Xi'an Jiaotong University, Xi'an 710049, China
[c] Helmholtz Institute Jena, D-07743 Jena, Germany
[d] Theoretisch-Physikalisches Institut, Friedrich-Schiller-University Jena, D-07743 Jena, Germany
[e] Key Laboratory of HEDP of the Ministry of Education, CAPT, State Key Laboratory of Nuclear Physics and Technology, Peking University, Beijing, 100871, China

Received 27 March 2018; revised 5 June 2018; accepted 25 June 2018
Available online 27 July 2018

Abstract

In this work, characteristics of X/γ-ray radiations by intense laser interactions with high-Z solids are investigated by means of a newly developed particle-in-cell (PIC) simulation code. The PIC code takes advantage of the recently developed ionization and collision dynamics models, which make it possible to model different types of materials based on their intrinsic atomic properties. Within the simulations, both bremsstrahlung and nonlinear Compton scatterings have been included. Different target materials and laser intensities are considered for studying the parameter-dependent features of X/γ-ray radiations. The relative strength and angular distributions of X/γ ray productions from bremsstrahlung and nonlinear Compton scatterings are compared to each other. The threshold under which the nonlinear Compton scatterings become dominant over bremsstrahlung is also outlined.

PACS Codes: 87.55.Gh; 52.25.Os

Keywords: Particle-in-cell simulations; Bremsstrahlung; Nonlinear Compton scattering; Laser-solid interactions

1. Introduction

Strong laser radiation, with intensity over 10^{20} W/cm^2, can nowadays be used to produce bright X/γ-ray radiation through the interaction with high-Z solid. The bright X/γ-ray radiation sources have many applications in several research areas [1–4]. For example, the bright X-ray burst can be used for high sensitivity imaging by Thomson scattering. Such γ-ray sources can also be used to the transmutation of nuclear waste through the (γ, *n*) reactions [5,6]. In addition, ultra bright γ-ray sources may help developing future γ–γ colliders [7], which are of fundamental importance for basic sciences.

When an intense laser beam irradiates a solid composed of high-Z materials, relativistic electrons can be produced in front of the target through the direct-laser-heating/acceleration mechanism [8–14]. These energetic electrons then propagate through the bulk solid and may trigger efficient bremsstrahlung emission. For a complete description of this electron transport and bremsstrahlung, different atomic and plasma processes need to be taken into account including ionization dynamics [15,16], collision dynamics [17–19], Ohm heating [20], as well as self-generated electromagnetic fields [21,22].

Until now, however, there is no comprehensive simulation model that can incorporate all the related physical processes.

* Corresponding author. State Key Laboratory of High Field Laser Physics, Shanghai Institute of Optics and Fine Mechanics, 201800 Shanghai, China.
E-mail address: wudong@siom.ac.cn (D. Wu).

https://doi.org/10.1016/j.mre.2018.06.002

Recently, we have developed a particle-in-cell (PIC) code, which enables us to calculate coupled atomic and plasma processes in a more realistic way. Indeed this PIC code provides us a good opportunity to investigate the X/γ-ray radiation of solid when irradiated by intense laser pulses. The PIC code takes advantage of the recently developed ionization [15] and collision [17] dynamics models. Within the simulations, the ionization charge state and conductivity (or resistivity) of target material evolve according to the local plasma and electromagnetic fields conditions. Therefore, different types of materials, like copper (Cu), gold (Au) and plastics, can be modelled based on their intrinsic atomic properties.

Bremsstrahlung is known as the dominant process in solids under intense laser irradiation, which typically results in a continuous and broad spectra. Although K_α and K_β emission might also appear in the radiation spectra, they are typically weak and of low frequencies when compared with bremsstrahlung radiation, especially when the laser intensity is over 10^{20} W/cm^2 [23]. By varying the target materials and laser intensities moreover, we can tune the energetic electrons' generation in front of the target and transport within the target. The "generation" and "transport" of electrons would act as a whole and finally influence the bremsstrahlung X/γ-ray emission. For laser intensities higher than 10^{23} W/cm^2, moreover, laser-plasma non-linearity, including the nonlinear Compton scatterings and radiation reactions effects [24,25], are predicted to appear. Such non-linear effects occur when relativistic electrons, quivering in the ultra intense electromagnetic fields, emit high frequency photons. Under such extreme conditions, the X/γ-rays from nonlinear Compton scatterings can become comparable to the bremsstrahlung radiation [26]. Furthermore, the radiation reaction effects of electrons can significantly influence the energetic electrons' generation in front of the target and even the following transport. Little is known, so far, about the bremsstrahlung radiation and nonlinear Compton scatterings at extreme laser irradiations, and how they need to be incorporated in order to model the total radiation of solid is still open. Therefore, a quantitative evaluation of radiation characteristics of different high-Z solids irradiated by intense laser pulses would be of significant importance for both basic science and engineering applications.

In this paper, the characteristics of X/γ-ray radiations by intense laser interactions with high-Z solids are investigated through particle-in-cell simulations. Within the simulations, both bremsstrahlung and nonlinear Compton scatterings have been included. In particular, we here have studied the relative strength and angular distributions of X/γ-ray productions from bremsstrahlung and nonlinear Compton scatterings. The threshold under which the nonlinear Compton scatterings become dominant is also outlined.

The paper is organized as follows. Our models concerning bremsstrahlung and nonlinear Compton scatterings are introduced in Sec. 2. In Sec. 3, PIC simulations concerning Cu and Au materials with laser of intensities varying from 10^{20} W/cm^2 to 10^{24} W/cm^2 are performed. The relative strength and angular distributions of X/γ-ray productions from bremsstrahlung and nonlinear Compton scatterings under different materials and laser irradiations are also compared in Sec. 3. Summary and discussion are given in Sec. 4.

2. Theoretical model

When two charged particles collide, they will accelerate in each other's electric field and as a result, emit electromagnetic waves. This kind of phenomenon is typically called bremsstrahlung radiation. Generally, the bremsstrahlung radiation power by an accelerated charge increases with $\dot{\beta}^2 Z^2$. This value is significantly determined by acceleration $\dot{\beta}$ and target atomic number Z. For different target materials, atomic number Z is changed accordingly. From the relation, $P \sim \dot{\beta}^2 Z^2$, it is apparent that high-Z material would be more preferable in X/γ-ray production. The energetic electrons produced in front of the target are mainly due to direct-laser acceleration mechanism. At extreme intensities, laser-plasma interactions become strongly nonlinear, where new and exotic phenomena are predicted to appear. Among the features of interest at this exotic quantum electro-dynamical regime are the so-called nonlinear Compton scatterings and the accompanied radiation reaction friction effects. They occur when relativistic electrons, quivering in the ultra intense electromagnetic fields, emit high frequency photons. In this section, we will give a brief introduction of the bremsstrahlung and nonlinear Compton scattering models used in our PIC simulations.

If we consider the energetic electron, for example E_k greater than MeV, projects into a high-Z solid, the bremsstrahlung radiation would become non-ignorable. Following the classical text by Jackson [27], we can obtain the energy radiated per unit length per unit frequency as,

$$\frac{\mathrm{d}^2E}{\mathrm{d}l\mathrm{d}(\hbar\omega)} = \frac{16}{3}\alpha r_\mathrm{e}^2 nA^2 \ln\left|\frac{2\gamma\gamma' m_\mathrm{e}c^2}{\hbar\omega}\right| \tag{1}$$

where n is the ion density of the target, A is the atomic number of the target material, $\alpha = e^2/\hbar c$ is fine structure constant, $r_\mathrm{e} = e^2/m_\mathrm{e}c^2$ is classical electron radius and $\gamma' = \gamma - \hbar\omega$ is the relativistic factor of the electron after the photon has been emitted. For energetic electrons, the radiation is emitted mainly in the forward direction, under the average angle $\sim 1/\gamma$ between the directions of motion of the electron and the emitted light. In PIC simulations, therefore, the angular distribution of emitted photons can be approximated as

$$\frac{\mathrm{d}E}{\mathrm{d}\Omega\mathrm{d}(\hbar\omega)} = \frac{4}{3\pi}\delta\left(1 - \frac{\boldsymbol{p}}{|\boldsymbol{p}|}\right)\alpha c r_\mathrm{e}^2 nA^2 \ln\left|\frac{2\gamma\gamma' m_\mathrm{e}c^2}{\hbar\omega}\right|\mathrm{d}t, \tag{2}$$

where a delta-function approximation is used in order to describe the direction of photon emissions.

In PIC simulations, as the average angle between photon and electron can be handled by a delta-function approximation, the Bremsstrahlung radiation do not further change the deflection of the electron. This approximation will significantly simplify the implementation of Bremsstrahlung correction into the binary collision models. In such model,

after the ordinary binary collision calculations, the electron energy is further updated by including the Bremsstrahlung correction, i.e., $\gamma_n = \gamma - \delta\gamma$ with $\delta\gamma$ representing the energy loss within collisions. The electron momentum is also updated with $\boldsymbol{p}_n = \sqrt{(\gamma_n - 1)/(\gamma - 1)}\boldsymbol{p}$, where δt is the time step of PIC simulations.

When an electron encounters strong electromagnetic fields, it can emit high frequency photons. This is called nonlinear Compton scatterings. In the meanwhile, this electron will lose much of its kinetic energy by radiation, and to which one usually refers as radiation reaction effects. In order to resolve this interaction, here, in our model [24,25,28], electrons are assumed to move in two separate fields: the original Lorenz field and its own radiated fields, as following,

$$\frac{\mathrm{d}\boldsymbol{p}}{\mathrm{d}t} = \boldsymbol{f}_\mathrm{L} + \left[\frac{e}{c}(\delta\boldsymbol{u} \times \boldsymbol{B}) - \frac{\boldsymbol{u}\gamma^2}{c^2}(\delta\boldsymbol{u} \cdot \boldsymbol{f}_\mathrm{L})\right], \tag{3}$$

where $\boldsymbol{f}_\mathrm{L}$ is the Lorenz force, $\boldsymbol{u} = \boldsymbol{p}/\sqrt{m^2 + \boldsymbol{p}^2/c^2}$, and $\delta\boldsymbol{u} = \frac{\tau}{m}\frac{\boldsymbol{f}_\mathrm{L} - \boldsymbol{u}(\boldsymbol{u}\cdot\boldsymbol{f}_\mathrm{L})/c^2}{1+\tau(\boldsymbol{u}\cdot\boldsymbol{f}_\mathrm{L})/mc^2}$, in which τ is a constant expressed as $\tau = 2e^2/3mc^3$. Again, the radiation direction is confined in a narrow angle $1/\gamma$ along the electron trajectory. In the highly relativistic case, it can also be approximated with the delta-function. The frequency spectrum can simply express as

$$\frac{dI}{\mathrm{d}\Omega\mathrm{d}\omega}\mathrm{d}t = \delta\left(\Omega - \frac{\boldsymbol{p}}{|\boldsymbol{p}|}\right)\frac{\gamma^2(\delta\boldsymbol{u}\cdot\boldsymbol{f}_\mathrm{L})}{\omega_\mathrm{c}}F(r)\mathrm{d}t, \tag{4}$$

with $F(r) = \frac{3^{5/2}}{8\pi}r\int_r^\infty K_{5/3}(x)\mathrm{d}x$, where $K_{5/3}$ is the modified Bessel function, $r = \omega/\omega_\mathrm{c}$, and $\omega_\mathrm{c} = 3\omega_\mathrm{r}\gamma^3/2$ is momentarily close to that from circular motion with a rotation frequency $\omega_\mathrm{r} = |\boldsymbol{p} \times \boldsymbol{f}_\mathrm{L}|/\boldsymbol{p}^2$.

Note that we have already implemented both bremsstrahlung and nonlinear Compton scatterings [25] into a PIC code [29]. When coupled with the ionization dynamics [15], collision dynamics [17], Ohm heating [20] as well as self-generated electromagnetic fields [21,22], the radiation properties of a high-Z solid under the irradiations of intense lasers can therefore also be calculated quantitatively.

3. Simulation results

We have performed a series of 2D PIC simulations to investigate the emitted spectra of Cu and Au targets, when irradiated by intense laser beams with intensities varying from 10^{20} W/cm^2 to 10^{24} W/cm^2. Here, Cu (density of 8.9 g/cm^3) and Au (density of 19.32 g/cm^3) targets with the same thickness 2 μm are used to analyse the effects of target material on radiation properties. The initial temperature of Cu and Au solid is chosen to be 0.01 eV. The initial ionization degrees of Cu and Au are $Z = 4$ and 5, respectively. We here take advantage of the recently developed ionization and collision dynamics models, which help calculate the ionization charge state and conductivity of target quite precisely according to the local plasma and electromagnetic fields conditions within the simulations. The simulations were carried out in the X-Y Cartesian geometry with laser propagation in the X direction. The size of the simulation box is chosen to be X (8 μm) × Y (20 μm), which is divided into 400 × 1000 uniform grids. The laser pulse has a predefined profile of form $\mathrm{e}^{-r^2/r_0^2}\sin^2(\pi t/2\tau_0)$, with $r_0 = 3\lambda_0$, $\tau_0 = 10T_0$ where T_0 is the laser cycle. The central wavelength of the laser is 1 μm. The laser pulse is normally incident on the target. In the X and Y directions, absorbing boundary conditions are applied for both particles and laser field. In order to quantitatively evaluate the radiation contributions from bremsstrahlung and nonlinear Compton scatterings, two separate simulation groups are performed: (a) taking into account the bremsstrahlung radiation only; (b) taking into account both bremsstrahlung radiation and nonlinear Compton scatterings.

Fig. 1 (a)–(c) shows the electron density profiles of Cu targets when irradiated by a laser pulse with intensity 10^{20} W/cm^2, 10^{23} W/cm^2 and 10^{24} W/cm^2, respectively. Here, snapshots of these densities are taken at the end of the laser pulses. Within these simulations (Fig. 1 (a)–(c)), only bremsstrahlung radiations are taken into account. In contrast, Fig. 1 (d)–(f) are the results when both bremsstrahlung and nonlinear Compton scatterings are involved. Fig. 2 shows that same for analogue parameters, but the Au targets are used instead of Cu. As seen from Fig. 1 (a), the laser beams cannot penetrate through the target with a laser of intensity 10^{20} W/cm^2, which are reflected back when reaching the critical density surfaces. The ionization channel inside the target is induced by energetic electrons, which are typically generated at the critical density surfaces and then propagate forward. From Figs. 1(a) and 2(a), we can see that the transport of energetic electrons is well guided inside both Cu and Au targets. The guiding of energetic electrons is proved to be the action of resistive magnetic fields [20–22], which are induced by Faraday's law $-\partial\boldsymbol{B}/\partial t = \nabla \times \boldsymbol{E}$ and Ohm's law $\boldsymbol{E} = \eta\boldsymbol{J}_\mathrm{e}$, where η is the resistivity of the bulk target and $\boldsymbol{J}_\mathrm{e}$ is the current density of slow moving backward electrons. The resistive magnetic fields will trend to collimate energetic electrons. This collimation counteracts the dispersion of electrons by collisions and other effects, like Weible and two-stream instabilities [30,31], within the transport. To evaluate the contribution of radiation reactions to electron dynamics, for intensity of 10^{20} W/cm^2, no significant contributions from radiation reactions have been seen from Figs. 1 and 2. These effects start to rise when laser intensity is increasing. When laser intensity reaches 10^{24} W/cm^2, the light pressure can penetrate through the whole solid target as in the hole-boring [32,33] regime. As seen from the comparison of Fig. 1 (c) and (f), the radiation reaction effects trend to prevent the target from breaking through.

In Fig. 3, we have summarized the totally emitted energy as a function of incident laser intensities. In general, the total emission energy increases monotonically with the laser intensity. For a Cu target, Fig. 3 (a) compares this total energy for two computations with and without nonlinear Compton scatterings. We can see that the contributions from nonlinear Compton scatterings appearing when laser intensities are larger than 10^{23} W/cm^2. At 10^{24} W/cm^2, nonlinear Compton scatterings can even become dominant over bremsstrahlung radiation. In contrast, in Fig. 3 (b), also at the laser intensity

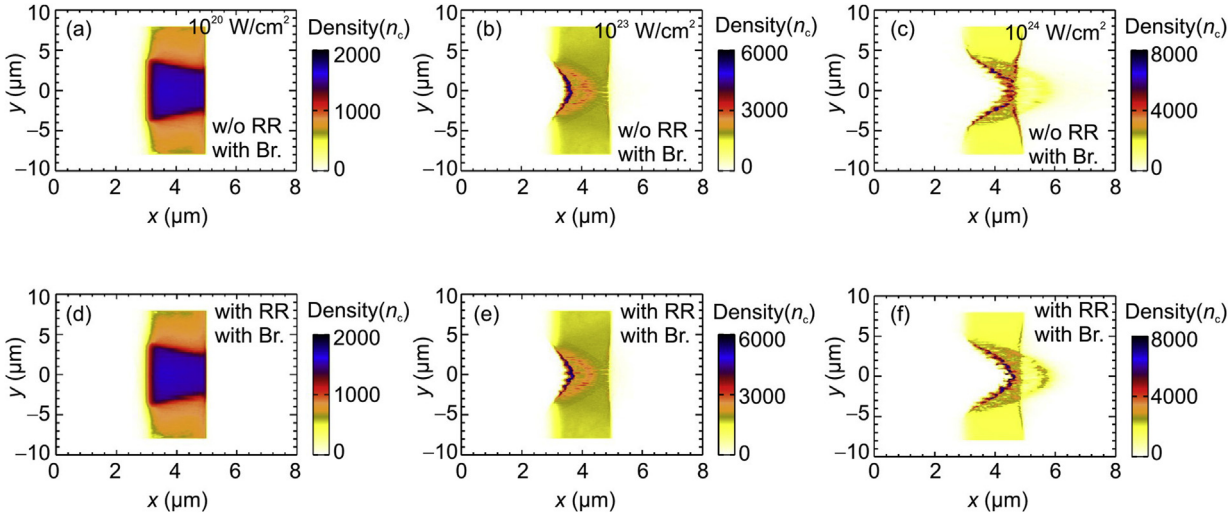

Fig. 1. The electron density profiles of copper (Cu) target when irradiated by intense laser pulses. The snapshots are taken at the end of laser pulses. (a)–(c) are the cases with laser of intensity 10^{20} W/cm^2, 10^{23} W/cm^2 and 10^{24} W/cm^2 if only the bremsstrahlung is included. (d)–(f) are the corresponding cases taken into account both bremsstrahlung and radiation reactions.

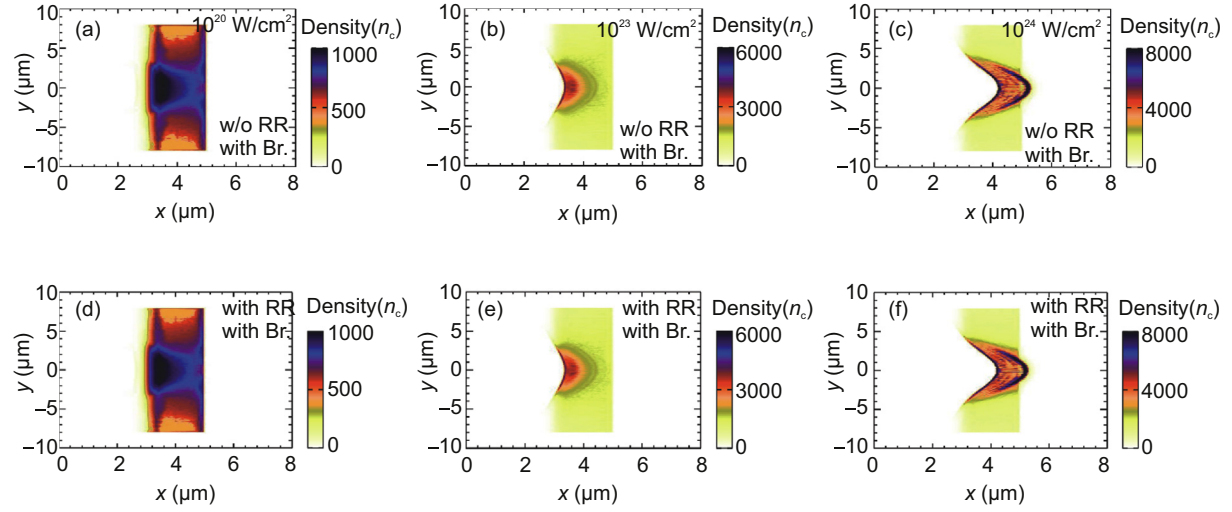

Fig. 2. The electron density profiles of gold (Au) target when irradiated by intense laser pulses. The snapshots are taken at the end of laser pulses. (a)–(c) are the cases with laser of intensity 10^{20} W/cm^2, 10^{23} W/cm^2 and 10^{24} W/cm^2 if only the bremsstrahlung is included. (d–f) are the corresponding cases when taken into account both bremsstrahlung and radiation reactions.

10^{24} W/cm^2, emitted energy from Au targets are presented. Even though the nonlinear Compton scattering plays important roles in the total radiations, it is still not dominant over bremsstrahlung. To be more specific, under laser irradiations with intensity 10^{24} W/cm^2, the total emitted energy from Cu targets when taking into account nonlinear Compton scatterings is increased from 0.3 unit to 0.7 unit. The net contribution from nonlinear Compton scatterings is 0.4 unit. While for the Au cases, it is increased from 0.8 unit to 0.9 unit. Here, the net contribution from nonlinear Compton scatterings is only 0.1 unit. Let us recall here that at laser intensity of 10^{24} W/cm^2, the Cu target is close to be broken through, while this is not at all the case for Au target. We can therefore conclude empirically the condition under which nonlinear Compton scatterings become dominant over bremsstrahlung—the laser intensity should be higher than 10^{23} W/cm^2 and simultaneously the laser beam should break through the target.

Fig. 4 displays the radiation spectra of Cu and Au targets when irradiated by intense laser beams with varying intensities. Here, dashed lines refer to the spectra in which only the bremsstrahlung is taken into account and show a broad distribution from 0 to a cut-off frequency. The cut-off frequency of bremsstrahlung is exactly the maximum kinetic energy of colliding electrons. While the radiation from nonlinear Compton scatterings are well peaked. The total radiation spectra are shown by solid lines, which taking into account both bremsstrahlung radiations and nonlinear Compton scatterings. As seen from Fig. 4 (a), at the laser intensity of 10^{23} W/cm^2, the peak spectra are relatively small compared with the broad bremsstrahlung spectra. While at laser intensity

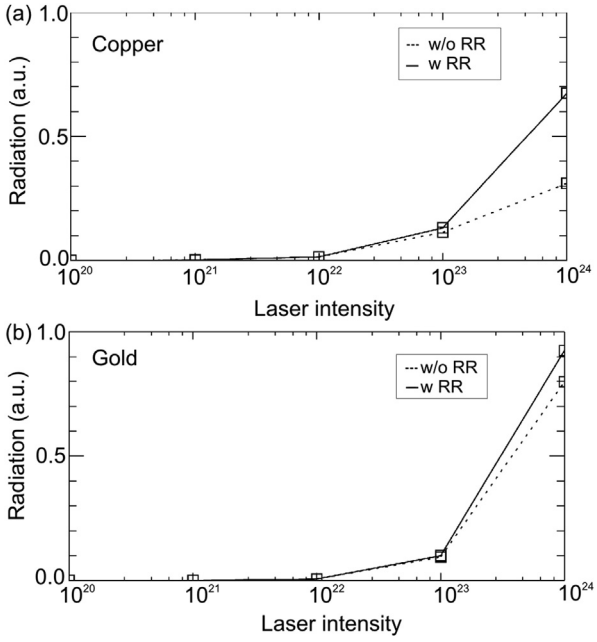

Fig. 3. The total energy of emitted photons as a function of laser intensities for (a) a copper and (b) gold target, respectively. Results are compared for only the bremsstrahlung (dashed line) and both the bremsstrahlung and nonlinear Compton scatterings (solid line) are taken into account.

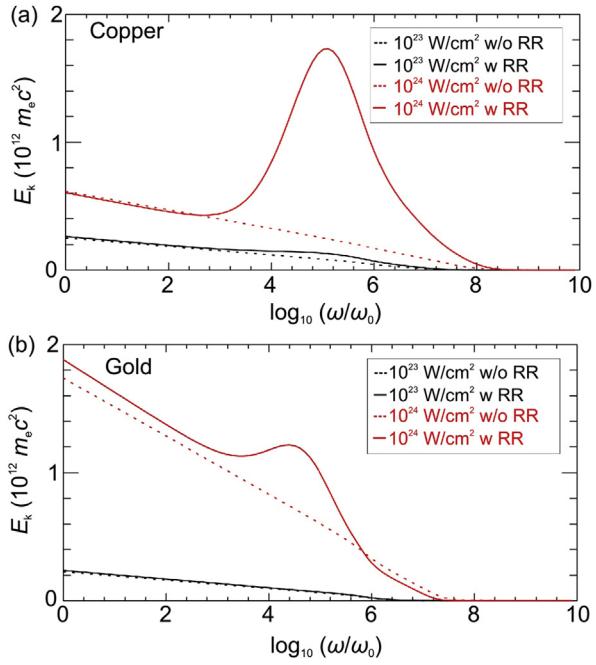

Fig. 4. The photon spectrum emitted from (a) Cu and (b) Au targets when irradiated by intense laser pulses with varying laser intensities. Here black lines correspond to laser intensity 10^{23} W/cm^2, and red lines are the cases of 10^{24} W/cm^2. While the dashed lines refer to simulations only taking into account the bremsstrahlung, and the solid lines describe simulations taking into account both the bremsstrahlung and nonlinear Compton scattering. Here, $1\omega_0 = 1.24$ eV.

10^{24} W/cm^2, the peak spectra is significantly dominant over the broad bremsstrahlung spectra. This behaviour is similar to the emitted radiation shown in Fig. 3. In contrast, in Fig. 4 (b), even at laser intensity 10^{24} W/cm^2, the contributions from nonlinear Compton scatterings is still not dominant over bremsstrahlung radiations. This is because, as shown in Fig. 2 (f), under these conditions, the Au target is not broken through.

Finally, Fig. 5 presents the angular distributions of emitted photons, where ϕ is defined as the angle between the X-axis and the photon propagation direction. Data from Cu and Au targets are shown in Fig. 5 (a) and (b), respectively. At laser intensity 10^{20} W/cm^2, the emission angular distributions of Cu shows two peaks, as seen from the blue line in Fig. 5 (a). One is located at 10°, the other at 160°. From these peaks, we find that most of the radiation is in the forward direction. The backward emission is due to the reflux of energetic electrons, which are drawn back by the sheath fields on the backside of the targets. The pretty good collimation of radiation can also be well explained by the guiding of resistive magnetic fields, as shown in Fig. 1 (a), where the photon and electron propagation directions almost coincide. In contrast, as shown in Fig. 5 (b), also under laser irradiation intensity 10^{20} W/cm^2, no significant collimation of radiation is found for Au targets. When referring to Fig. 2 (a), we find the reason. Although the resistive magnetic fields also play roles in the transport processes, in the Au cases, it is several times higher. This is because the resistive magnetic field is significantly determined by resistivity, which is proportional to the average charge state Z. A large resistive magnetic field will first collimate the

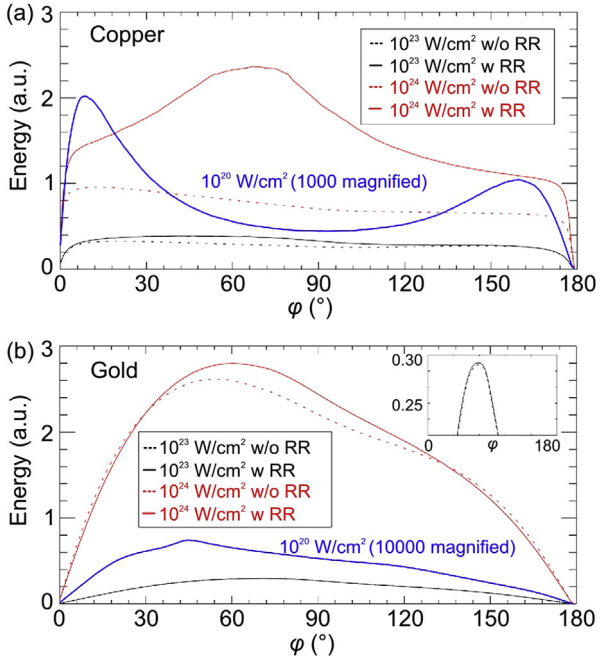

Fig. 5. The angular distribution of the emitted photons from (a) Cu and (b) Au targets irradiated by intense laser pulses with varying laser intensities. Here black lines correspond to laser intensity 10^{23} W/cm^2, red lines are the cases of 10^{24} W/cm^2 and blue lines are the cases of 10^{20} W/cm^2. The dashed and solid lines refer to the same computational model as in Fig. 4. For laser intensity 10^{20} W/cm^2, as the contribution of nonlinear Compton scattering is extremely small, the dashed and solid lines are merged as single solid lines. The inset of (b) is the magnified comparison when including and excluding nonlinear Compton scatterings, for laser intensity 10^{23} W/cm^2.

energetic electrons and later diverge them. These two counter-interacting effects will finally lead to larger emission angles. When laser intensity becomes higher, the angular distributions of emitted photons become much complicated. Even though, we still notice some quantitative features of angular distributions from bremsstrahlung and nonlinear Compton scatterings. From the comparison of the solid red line and dashed red line in Fig. 5 (a), we therefore see the direction of bremsstrahlung radiation to be forward, while the direction of nonlinear Compton scatterings to be along the laser polarization directions, i.e. 90°.

4. Discussion and conclusions

Note that when the laser pulses are obliquely incident to solid targets [34], the interaction will present further complexity. Although such cases are closely related to real experiments, they are, at present, out of the contents of this work, and might be addressed somewhere else in the near future.

To summarize, characteristics of X/γ-ray radiations by intense laser interactions with high-Z solids have been investigated by means of our recently developed PIC simulation code. This PIC code takes advantage of the newly developed ionization and collision dynamics models. Within the simulations, the ionization charge state and conductivity of target can therefore evolve quite precisely according to the local plasma and electromagnetic fields conditions. Different types of materials can be modelled due to their intrinsic atomic properties. Along with ionization and collision dynamics, bremsstrahlung and nonlinear Compton scatterings have also been included in the simulations. In this work, simulations with different target materials (Cu vs. Au) and varying laser intensities are performed to study the parameter-dependent features of X/γ-ray radiations. The relative strength and angular distributions of X/γ-ray production from bremsstrahlung and nonlinear Compton scatterings are compared to each other, and a threshold is determined under which the nonlinear Compton scattering is dominant.

Conflict of interest

There are no conflicts of interest.

Acknowledgments

This work was supported by Science Challenge Project (No. TZ2016005), National Natural Science Foundation of China (No. 11605269, 11674341 and 11675245) and National Basic Research Program of China (Grant No. 2013CBA01504).

References

[1] C. Wang, X.-T. He, P. Zhang, Ab initio simulations of dense helium plasmas, Phys. Rev. Lett. 106 (2011), 145002.
[2] M. Roth, T.E. Cowan, M.H. Key, S.P. Hatchett, C. Brown, et al., Fast ignition by intense laser-accelerated proton beams, Phys. Rev. Lett. 86 (2001) 436.
[3] T.Z. Esirkepov, S.V. Bulanov, K. Nishihara, T. Tajima, F. Pegoraro, et al., Proposed double-layer target for the generation of high-quality laser-accelerated ion beams, Phys. Rev. Lett. 89 (2002), 175003.
[4] Boris Yu. Sharkov, Dieter H.H. Hoffmann, Alexander A. Golubev, Yongtao Zhao, High energy density physics with intense ion beams, Matter Radiat. Extr. 1 (2016) 28.
[5] J. Magill, H. Schwoerer, F. Ewald, J. Galy, R. Schenkel, et al., Laser transmutation of iodine-129, Appl. Phys. B 77 (2003) 387.
[6] E. Irani, H. Omidvar, R. Sadighi-Bonabi, Gamma rays transmutation of Palladium by bremsstrahlung and laser inverse Compton scattering, Energy Convers. Manage. 77 (2014) 558.
[7] O.J. Pike, F. Mackenroth, E.G. Hill, S.J. Rose, A photonCphoton collider in a vacuum hohlraum, Nat. Photon. 8 (2014) 434.
[8] B.S. Paradkar, M.S. Wei, T. Yabuuchi, R.B. Stephens, M.G. Haines, et al., Numerical modeling of fast electron generation in the presence of preformed plasma in laser-matter interaction at relativistic intensities, Phys. Rev. E 83 (2011), 046401.
[9] B.S. Paradkar, S.I. Krasheninnikov, F.N. Beg, Mechanism of heating of pre-formed plasma electrons in relativistic laser-matter interaction, Phys. Plasmas 19 (2012), 060703.
[10] S.I. Krasheninnikov, Stochastic heating of electrons by intense laser radiation in the presence of electrostatic potential well, Phys. Plasmas 21 (2014), 104510.
[11] D. Wu, S.I. Krasheninnikov, S.X. Luan, W. Yu, Identifying the source of super-high energetic electrons in the presence of pre-plasma in laser-matter interaction at relativistic intensities, Nucl. Fusion 57 (2017), 016007.
[12] D. Wu, S.I. Krasheninnikov, S.X. Luan, W. Yu, The controllable super-high energetic electrons by external magnetic fields at relativistic laser-solid interactions in the presence of large scale pre-plasmas, Phys. Plasmas 23 (2016), 123116.
[13] D. Wu, S.X. Luan, J.W. Wang, W. Yu, J.X. Gong, et al., The controllable electron-heating by external magnetic fields at relativistic laser-solid interactions in the presence of large scale pre-plasmas, Plasma Phys. Control. Fusion 59 (2017), 065004.
[14] S.M. Weng, Z.M. Sheng, M. Murakami, M. Chen, M. Liu, et al., Optimization of hole-boring radiation pressure acceleration of ion beams for fusion ignition, Matter Radiat. Extr. 3 (2018) 28.
[15] D. Wu, X.T. He, W. Yu, S. Fritzsche, Monte Carlo approach to calculate ionization dynamics of hot solid-density plasmas within particle-in-cell simulations, Phys. Rev. E 95 (2017), 023208.
[16] D. Wu, B. Qiao, C. McGuffey, X.T. He, F.N. Beg, Generation of high-energy mono-energetic heavy ion beams by radiation pressure acceleration of ultra-intense laser pulses, Phys. Plasmas 21 (2014), 123118.
[17] D. Wu, X.T. He, W. Yu, S. Fritzsche, Monte Carlo approach to calculate proton stopping in warm dense matter within particle-in-cell simulations, Phys. Rev. E 95 (2017), 023207.
[18] K. Nanbu, S. Yonemura, Weighted particles in Coulomb collision simulations based on the theory of a cumulative scattering angle, J. Comput. Phys. 145 (1998) 639.
[19] Y. Sentoku, A.J. Kemp, Numerical methods for particle simulations at extreme densities and temperatures: weighted particles, relativistic collisions and reduced currents, J. Comput. Phys. 227 (2008) 6846.
[20] P. Leblanc, Y. Sentoku, Scaling of resistive guiding of laser-driven fast-electron currents in solid targets, Phys. Rev. E 89 (2014), 023109.
[21] Y. Sentoku, E. dHumieres, L. Romagnani, P. Audebert, J. Fuchs, Dynamic control over mega-ampere electron currents in metals using ionization-driven resistive magnetic fields, Phys. Rev. Lett. 107 (2011), 135005.
[22] L.G. Huang, T. Kluge, T.E. Cowan, Dynamics of bulk electron heating and ionization in solid density plasmas driven by ultra-short relativistic laser pulses, Phys. Plasmas 23 (2016), 063112.
[23] F. Zamponi, A. Lubcke, T. Kampfer, I. Uschmann, E. Forster, et al., Directional bremsstrahlung from a Ti laser-produced X-ray source at

relativistic intensities in the 3C12 keV range, Phys. Rev. Lett. 105 (2010), 085001.
[24] Igor V. Sokolov, Natalia M. Naumova, John A. Nees, Gerard A. Mourou, Victor P. Yanovsky, Radiation back-reaction in relativistically strong and QED-strong pulsed laser fields, Phys. Plasmas 16 (2009), 093115.
[25] D. Wu, B. Qiao, X.T. He, The radiation reaction effects in the ultra-intense and ultra-short laser foil interaction regime, Phys. Plasmas 22 (2015), 093108.
[26] F. Wan, C. Lv, M. Jia, H. Sang, B.S. Xie, Photon emission by bremsstrahlung and nonlinear Compton scattering in the interaction of ultra-intense laser and plasmas, Eur. Phys. J. D 71 (2017) 236.
[27] J.D. Jackson, Classical Electrodynamics, Wiley & Sons, New York, 1999.
[28] Zheng Gong, Ronghao Hu, Yinren Shou, Bin Qiao, Chiaer Chen, et al., Radiation reaction induced spiral attractors in ultra-intense colliding laser beams, Matter Radiat. Extr. 1 (2016) 308.
[29] H. Xu, W.W. Chang, H.B. Zhuo, L.H. Cao, Z.W. Yue, Parallel programming of 2(1/2)-dimensional PIC under distributed-memory parallel environments, Chin. J. Comput. Phys. 19 (2002) 305.
[30] Qing Jia, Hong-bo Cai, Wei-wu Wang, Shao-ping Zhu, Z.M. Sheng, et al., Effects of the background plasma temperature on the current filamentation instability, Phys. Plasmas 20 (2013), 032113.
[31] S.V. Bulanov, T. Zh. Esirkepov, M. Kando, F. Pegoraro, S. Bulanov, et al., Ion acceleration from thin foil and extended plasma targets by slow electromagnetic wave and related ion-ion beam instability, Phys. Plasmas 19 (2012), 103105.
[32] D. Wu, C.Y. Zheng, C.T. Zhou, X.Q. Yan, M.Y. Yu, et al., Suppressing longitudinal double-layer oscillations by using elliptically polarized laser pulses in the hole-boring radiation pressure acceleration regime, Phys. Plasmas 20 (2013), 023102.
[33] D. Wu, C.Y. Zheng, B. Qiao, C.T. Zhou, X.Q. Yan, et al., Suppression of transverse ablative Rayleigh-Taylor-like instability in the hole-boring radiation pressure acceleration by using elliptically polarized laser pulses, Phys. Rev. E 90 (2014), 023101.
[34] Z.M. Sheng, Y. Sentoku, K. Mima, J. Zhang, W. Yu, et al., Angular distributions of fast electrons, ions, and bremsstrahlung X/γ-rays in intense laser interaction with solid targets, Phys. Rev. Lett. 85 (2000) 5340.